

Design, synthesis, molecular modeling and neuroprotective effects of a new framework of cholinesterase inhibitors for Alzheimer's disease

Vanessa S. Zanon , Josélia A. Lima , Rackele F. Amaral , Flavia R. S. Lima , Daniel A. S. Kitagawa , Tanos C. C. França & Maria D. Vargas

To cite this article: Vanessa S. Zanon , Josélia A. Lima , Rackele F. Amaral , Flavia R. S. Lima , Daniel A. S. Kitagawa , Tanos C. C. França & Maria D. Vargas (2020): Design, synthesis, molecular modeling and neuroprotective effects of a new framework of cholinesterase inhibitors for Alzheimer's disease, Journal of Biomolecular Structure and Dynamics, DOI: [10.1080/07391102.2020.1796796](https://doi.org/10.1080/07391102.2020.1796796)

To link to this article: <https://doi.org/10.1080/07391102.2020.1796796>

 View supplementary material 

 Published online: 25 Jul 2020.

 Submit your article to this journal 

 View related articles 

 View Crossmark data 



Design, synthesis, molecular modeling and neuroprotective effects of a new framework of cholinesterase inhibitors for Alzheimer's disease

Vanessa S. Zanon^a , Josélia A. Lima^{b,c} , Rackele F. Amaral^d , Flavia R. S. Lima^d , Daniel A. S. Kitagawa^c , Tanos C. C. França^c  and Maria D. Vargas^a 

^aInstituto de Química, Universidade Federal Fluminense, Niterói, RJ, Brazil; ^bPrograma de Pós-graduação em Saúde do Adulto, Universidade Federal do Maranhão, São Luís, MA, Brazil; ^cLaboratório de Modelagem Aplicada a Defesa Química e Biológica (LMDQB), Instituto Militar de Engenharia, Rio de Janeiro, RJ, Brasil; ^dLaboratório de Biologia das Células Gliais, Instituto de Ciências Biomédicas, Centro de Ciências da Saúde, Universidade Federal do Rio de Janeiro, Rio de Janeiro, RJ, Brasil

Communicated by Ramaswamy H. Sarma

ABSTRACT

In search of a novel class of compounds against Alzheimer's disease (AD), a new series of 7-chloro-aminoquinoline derivatives containing methylene spacers of different sizes between the 7-chloro-4-aminoquinoline nucleus and imino methyl substituted phenolic rings, and also their reduced analogues, were designed, synthesized and evaluated as neuroprotective agents for AD *in vitro*. In spite of the multifaceted feature of AD, cholinesterases continue to be powerful and substantial targets, as their inhibition increases both the level and duration of the acetylcholine neurotransmitter action. The compounds presented inhibitory activity in the micromolar range against acetylcholinesterase (AChE) (imines and amines) and butyrylcholinesterase (BChE) (amines). The SAR study revealed that elongation of the imine side chain improved AChE activity, whereas the reduction of these compounds to amines was crucial for higher activity and indispensable for BChE inhibition. The most promising selective inhibitors were not cytotoxic and did not stimulate pro-inflammatory activity in glial cells. Kinetic and molecular modeling studies indicated that they also show mixed-type inhibition for both enzymes, behaving as dual-site inhibitors, which can interact with both the peripheral anionic site and the catalytic anionic site of AChE. They could therefore restore cholinergic transmission and also may inhibit the aggregation of A β promoted by AChE. Additionally, one compound showed promising anti-inflammatory activity by reducing the microglial release of NO \bullet at a concentration that is equivalent to the IC₅₀ against BChE (30.32 \pm 0.18 μ M) and 15-fold greater than the IC₅₀ against AChE (1.97 \pm 0.20 μ M).

ARTICLE HISTORY

Received 5 May 2020
Accepted 13 July 2020

KEYWORDS

Acetylcholinesterase; butyrylcholinesterase; Alzheimer's disease; 7-chloro-4-aminoquinoline derivatives; neuroprotection; neuroinflammation

Introduction

Alzheimer's disease (AD) is a fatal disorder characterized by marked atrophy of the cerebral cortex and loss of basal forebrain cholinergic neurons (Mesulam, 2009). The major pathological features of AD are related to neuronal degeneration and include extracellular deposition of amyloid beta (A β) plaques, intracellular formation of neurofibrillary tangles, which are made up of hyperphosphorylated tau protein, and neuroinflammation (Guzmán-Martínez et al., 2013; Millington et al., 2014).

Recent technological progress made possible the development of tests and techniques to diagnose AD even at the prodromal stage, when early symptoms emerge. 'Biomarker' tests like those searching for A β and tau proteins in the blood and cerebrospinal fluid and also functional imaging techniques, such as specialized positron emission tomography and magnetic resonance imaging scans (Caldwell et al., 2015) have emerged, opening the possibility for an eventual intervention in the preclinical stage of AD. In

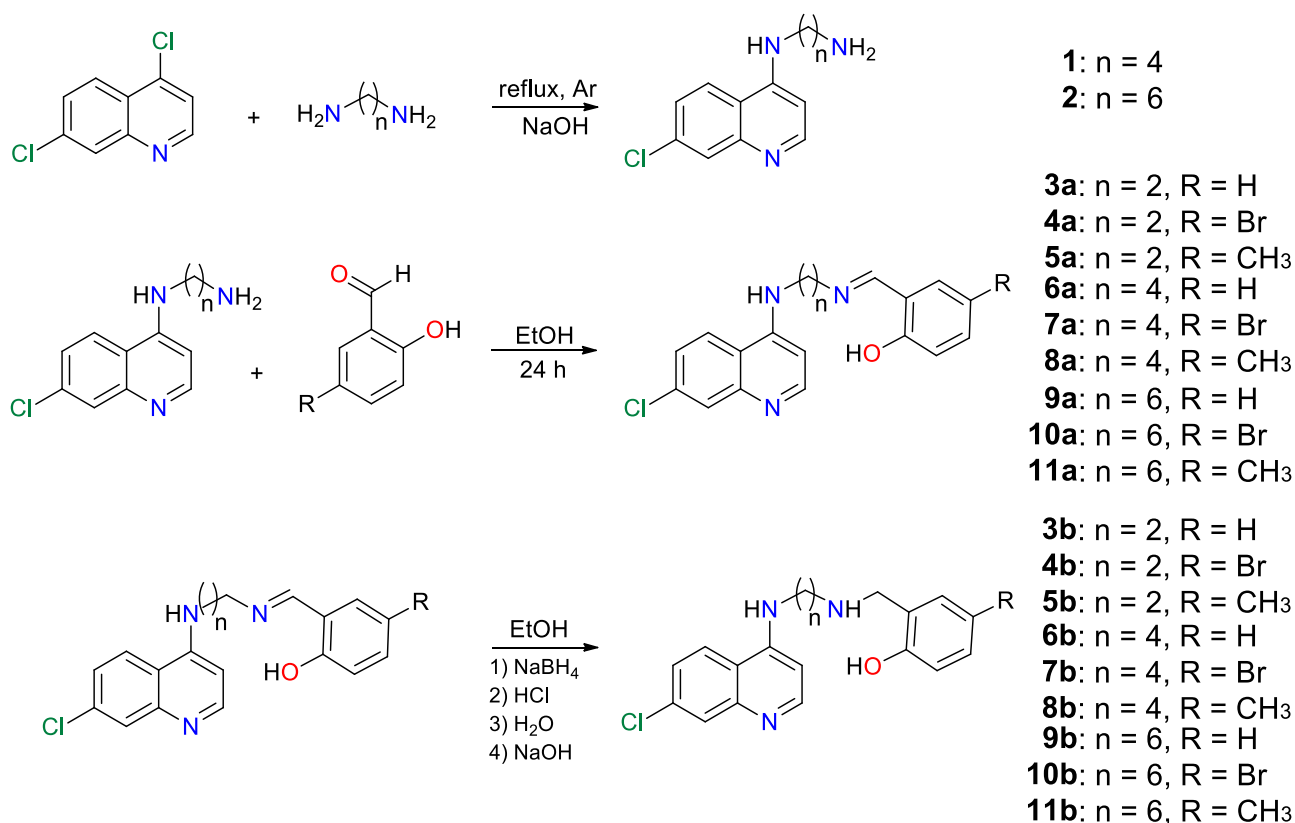
contrast, the current available drug therapy consisting of three anticholinesterase drugs (galantamine, donepezil and rivastigmine) and an N-methyl-D-aspartate receptor antagonist (memantine) is not effective in disrupting the progression of established AD and is unable to address the multifactorial nature of AD. Therefore, it is imperative to discover new drugs capable of restoring neurotransmission and preventing the processes that lead to neurodegeneration. The design and synthesis of compounds guided by biological assays has been an important tool in the search for effective multitarget drug candidates.

The quinoline nucleus is an important natural and synthetic class of heterocyclic compounds well known for having a broad spectrum of pharmacological activities, such as anti-cancer, anti-tubercular, anti-fungal, anti-convulsant, anti-inflammatory, cardiovascular activities, anti-bacterial, anti-viral, anti-obesity and anti-malarial (Hastings et al., 2002; Kumar et al., 2009; Marella et al., 2013). Only a few compounds containing a quinoline ring have been investigated in the context of AD (Ikram et al., 2012; Mantoani et al.,

CONTACT Josélia A. Lima  joselialima@terra.com.br  Programa de Pós-graduação em Saúde do Adulto, Universidade Federal do Maranhão, São Luís, MA, Brazil; Maria D. Vargas  mdvargas@id.uff.br  Instituto de Química, Universidade Federal Fluminense, Niterói, RJ, Brazil

 Supplemental data for this article can be accessed online at <https://doi.org/10.1080/07391102.2020.1796796>

© 2020 Informa UK Limited, trading as Taylor & Francis Group



Scheme 1. Synthesis of 7-chloro-4-aminoquinoline derivatives **1**, **2**, **3a–11a** and **3b–11b**.

2016) and the 4-aminoquinoline nucleus has been shown to be a good starting core for the design of novel cholinesterase inhibitors (Chen et al., 2016).

We recently reported (Zanon et al., 2019) the first 7-chloro-4-aminoquinoline derivatives (HL) with acetylcholinesterase (AChE) inhibitory activity (**3a–5a**, see Scheme 1), which motivated us to continue working on this template as a strategy to obtain more potent compounds able to inhibit both AChE and butyrylcholinesterase (BChE) and that may serve as prototypes for the development of drugs for the different stages of AD.

Herein we report the design, synthesis, molecular docking, the cholinesterase inhibitory activities, including the kinetic studies, neurotoxicity and neuroprotection of a new series of imines containing the 7-chloro-4-aminoquinoline nucleus **3a–11a** and their reduced amine derivatives **3b–11b** (Scheme 1).

Results and discussion

Chemistry

Considering the good AChE inhibition activity of imines **3a**, **4a** and **5a** (Scheme 1; Zanon et al., 2019), we decided to explore further this hybrid skeleton to investigate the influence of the alkyl side chain length on the activity. Hence the reactions of diamines **1** and **2** with the substituted salicylaldehydes ($R = H, Br$ and CH_3) in ethanol yielded the Schiff bases **3a–11a** in fair to excellent yields (36–81%). In order to confer higher flexibility and improve their solubility, these compounds were subsequently reduced to the corresponding secondary amines **3b–11b** (42–96%) by using sodium

borohydride in ethanol (Scheme 1). All compounds were characterized by physical (melting point), spectral (1H and ^{13}C NMR and IR spectroscopy; supporting information Figures S1–S45) and analytical (elemental analysis) data (see Experimental section).

The presence of a singlet around δ 8.40, attributed to the imine proton in the 1H NMR spectra of **3a–11a**, confirmed the synthesis of the imines. The disappearance of this peak and the appearance of a singlet between δ 3.9–4.1 in the spectra of **3b–11b** confirmed the reduction of the compounds. In all spectra, the aromatic protons of the 7-chloroquinoline and the phenol rings appeared between δ 6.3 and 8.6 and the aliphatic protons, at δ 3.7–1.4. The aromatic and aliphatic carbons appeared, respectively, at δ 155.0–99.6 and δ 58.6–19.8 in the ^{13}C NMR spectra of all compounds, whereas the carbon resonance frequency of the $CH=N$ group was detected at δ 164.8–167.0 in the spectra of imines. In the IR spectra of **3a–11a**, the characteristic imine $C=N$ stretching vibration was observed around 1630 cm^{-1} and was absent in the spectra of the reduced compounds **3b–11b**. Furthermore all compounds exhibited the bands associated to the 7-chloroquinoline nucleus, including the strong $C=N$ band, at around 1610, and $C=C$ bands at 1580 and 1540 cm^{-1} (Ekengard et al., 2015).

Cholinesterases inhibitory activities

In our recent report (Zanon et al., 2019) we showed that all the investigated 7-chloro-4-aminoquinoline derivatives (of which **3a–5a**, Table 1) presented interesting specific

Table 1. IC₅₀ values of *Ee*AChE and *Eq*BChE inhibition of compounds **3a–11a** and **3b–11b**.

Compound	<i>n</i>	<i>R</i>	<i>Ee</i> AChE IC ₅₀ ^a (μM)	<i>Eq</i> BChE IC ₅₀ ^a (μM)	Selectivity for <i>Ee</i> AChE ^b
3a ^c	2	H	4.61 ± 0.48	>100	–
4a ^c	2	Br	7.17 ± 0.43	>100	–
5a ^c	2	CH ₃	7.34 ± 0.06	>100	–
6a	4	H	5.51 ± 0.59	>100	–
7a ^d	4	Br	–	–	–
8a	4	CH ₃	3.06 ± 0.27	>100	–
9a	6	H	0.73 ± 0.04	58.38 ± 5.52	80.0
10a	6	Br	3.65 ± 0.04	>100	–
11a	6	CH ₃	2.25 ± 0.08	33.47 ± 1.36	14.9
3b	2	H	1.97 ± 0.20	30.32 ± 0.18	15.4
4b	2	Br	24.17 ± 2.10	21.54 ± 0.64	0.9
5b	2	CH ₃	1.70 ± 0.08	8.39 ± 0.26	4.9
6b	4	H	0.57 ± 0.03	8.15 ± 0.11	14.3
7b	4	Br	1.01 ± 0.15	2.77 ± 0.39	2.7
8b	4	CH ₃	0.99 ± 0.05	7.47 ± 0.33	7.5
9b	6	H	0.26 ± 0.01	6.13 ± 0.75	23.6
10b	6	Br	0.26 ± 0.05	1.75 ± 0.14	6.8
11b	6	CH ₃	0.26 ± 0.02	1.58 ± 0.01	6.1
Tacrine			0.041 ± 0.0002	0.0045 ± 0.0005	1.1
Donepezil ^e			0.035 ± 0.003	2.32 ± 0.10	66.3
Galantamine ^e			2.67 ± 0.18	12.7 ± 0.3	4.8

^aIC₅₀: 50% inhibitory concentration (means ± SD of three experiments, each one in three replicates).

^bSelectivity for *Ee*AChE is determined as ratio *Eq*BChE IC₅₀/*Ee*AChE IC₅₀.

^cZanon et al. (2019).

^dInsoluble.

^eLi et al. (2016).

inhibition of *Electrophorus electricus* AChE (*Ee*AChE) activity, with IC₅₀ values varying from 4.61 to 9.31 μM. These results inspired us to continue working on this template, and therefore, based on the most potent compounds (**3a**, **4a** and **5a**), we developed a series of imines containing different methylene spacers (*n* = 4 and 6; *R* = H, Br and CH₃) between the quinoline nucleus and the phenolic ring (compounds **6a–11a**), and also a series of their reduced analogues (compounds **3b–11b**; Scheme 1), in order to evaluate the contribution of the double bond of the imine to the inhibitory potency of the compounds. Enzymes of non-human origin namely *Ee*AChE and Equine serum BChE (*Eq*BChE) were used for the screening, because of their lower cost and high degree of similarity with their respective human enzymes. The results are shown in Table 1.

The results reveal that the presence of a six-methylene spacer (*n* = 6) in place of the ethylene or butylene (*n* = 2, 4) ones resulted in significant increase of the inhibitory potency of all compounds. Thus, imines **9a**, **10a** and **11a** (*n* = 6) were, respectively, 6, 2 and 3 times more potent AChE inhibitors than imines **3a**, **4a** and **5a** (*n* = 2), and amines **9b**, **10b** and **11b** (*n* = 6) were 8, 93 and 6 times better AChE inhibitors than compounds **3b**, **4b** and **5b** (*n* = 2), respectively. Furthermore, imines with two and four methylene spacers inhibited only AChE, whereas except for **10a**, those with a six-methylene spacer, **9a** and **11a**, inhibited both AChE and BChE in a concentration-dependent manner. The anticholinesterase potency of donepezil-based agents (Li et al., 2016) and *o*-hydroxyl-benzylamine-tacrine hybrids (Mao et al., 2012) has been previously associated to the spacer length.

In general, the amines were the most potent AChE inhibitors and differently from the imines, they all inhibited both AChE and BChE. The effect of the double bond on the

enzymatic selectivity of the compounds is clear when comparing the inhibitory activities of amines **3b**, **4b** and **5b** and imines **3a**, **4a** and **5a**. The amines inhibited both enzymes in a concentration-dependent manner and were more selective for AChE, with the exception of **4b**, which showed nonselective inhibition. Furthermore, the larger the size of the amine spacer, the higher was the inhibitory potency of the amines for both enzymes, independently of the substituent (*R* = H, IC₅₀ values for **9b** < **6b** < **3b**; *R* = Br, IC₅₀ values for **10b** < **7b** < **4b** and *R* = CH₃, IC₅₀ values of **11b** < **8b** < **5b**).

The data in Table 1 show no clear correlation between the nature of the substituent and the inhibitory activity of both imines and amines. In general, the unsubstituted imines containing two- and six-methylene spacers (**3a** and **9a**) were better AChE inhibitors than their substituted counterparts (**4a**, **5a** and **10a**, **11a**, respectively). However, the six-methylene spacer CH₃-substituted imine **11a** was better BChE inhibitor than the unsubstituted **9a**.

For the amines, the nature of the *R* group has little or no influence on the AChE inhibition potency of the compounds, except for those containing two-methylene spacers, which we associate to the low solubility of **4b** (*R* = Br) compared with **3b** and **5b**. In contrast, *R*-substituted amines were better BChE inhibitors than the unsubstituted ones, independently of the spacer. CH₃-substituted amines containing two- and six-methylene spacers (**5b** and **11b**, respectively) were the most active compounds of each series, whereas of the amines containing the four-methylene spacer, the Br-substituted compound (**7b**) was the most potent inhibitor.

None of the compounds was better cholinesterase inhibitor than tacrine (Table 1), but they present inhibitory profiles close to those found for donepezil and galantamine in the same enzymatic species evaluated in this work (Li et al., 2016). Compounds **7b**, **10b** and **11b** were as effective in inhibiting BChE as donepezil, while compounds **5b–11b** were all more potent inhibitors of AChE and BChE than galantamine.

The results show that the experimental design performed to increase the inhibitory activity of the compounds was quite satisfactory. In general, both the reduction of the double bond and the increase of the alkyl chain have been shown to contribute to the increase of the inhibitory potency of the compounds.

It has been reported that during the development of AD the BChE activity increases by 40–90% in the temporal cortex and hippocampus, whereas at the same time AChE activity decreases by up to 45% (Greig et al., 2001; Guillozet et al., 1997). Consequently, both AChE and BChE are important targets in the therapy of AD. Thus, compounds capable of inhibiting one or both of the enzymes are interesting prototypes for the development of anti-AD drugs. For this reason, we chose for further studies the compounds with IC₅₀ values ≤ 2 μM, that is, **9a**, **3b**, **5b–11b**. All were more selective for AChE (Table 1) in the following order of selectivity: **9a** (80×), **9b** (24×), **3b** (15×), **6b** (14×), **8b** and **10b** (7×), **11b** (6×), **5b** (5×), **7b** (3×).

Toxic effects on glial cells

Astrocytes, the most abundant cell type in the central nervous system (CNS), are crucial for the development and

maintenance of neurons in the brain (Stellwagen et al., 2019; Valori et al., 2019). Astrocyte cultures were treated with different concentrations of the compounds, which were selected based on the half maximal inhibitory concentration (IC_{50}) values for the inhibition of AChE and BChE, including concentrations that are lower than and 10 times higher than the IC_{50} value for AChE and at least twice higher than the IC_{50} value for BChE, for 24 and 48 h. The cells remained viable in the presence of all compounds at the IC_{50} values for AChE, both after 24 and 48 h of treatment (Figure 1(a–i)). Compounds **9a** (100 μ M), **3b** (60 μ M), **5b** (20 μ M), **10b** (30 μ M) and **11b** (10 and 30 μ M) impaired the viability of astrocytes only at twice or more the IC_{50} value or higher for BChE (Figure 1(a–c and h), respectively). Compounds **6b** (6, 8 and 16 μ M), **7b** (5 and 10 μ M), **8b** (8, 10 and 16 μ M) and **9b** (10 and 30 μ M), however, were toxic to astrocytes at the concentration close to the BChE inhibitory IC_{50} value (Figure 1(d–g, i)).

N9 microglial lineage activation

Microglial cells, the CNS defense cells, were used for this experiment. Microglial activation was analyzed for nitric oxide ($NO\bullet$) production after 48 h incubation with compounds that showed no toxic effects at their AChE and BChE inhibitory IC_{50} values (**9a**, **3b**, **5b** and **10b**; Figure 2). The concentrations used for this experiment were defined as 10 times the IC_{50} values for AChE and once that of BChE. Lipopolysaccharides (LPS) were used as positive control of nitric oxide release. N9 microglial lineage cells were viable during the experiment performance. This result suggests that the compounds were unable to induce activation of microglial cells and promote pro-inflammatory responses through secretion of neurotoxic factors, such as $NO\bullet$, and did not present anti-inflammatory activity, except for **3b** that showed the ability to reduce $NO\bullet$ release at 30 μ M. Thus, this compound shows promising anti-inflammation activity.

Kinetics of enzyme inhibition

To determine the mechanism of enzyme inhibition, kinetic studies were performed using **3b** as representative compound (Figure 3). The relative velocity of the enzyme was determined at 6 increasing concentrations of the substrate, in the absence and presence of the inhibitor. The mechanism of inhibition was graphically determined by applying the Lineweaver–Burk plot, using the reciprocal of velocity and substrate concentration. Based on the plots obtained for both substrates, acetylthiocholine iodide (ATCI) and butyrylthiocholine iodide (BTCl), a mixed-type inhibition mechanism was established for the compound (Figure 3, left). Using the Lineweaver–Burk secondary plot (Figure 3, right), K_i values were obtained.

The pattern of the Lineweaver–Burk plots indicated that **3b** is a mixed-type inhibitor of AChE ($K_i = 3.05 \mu$ M) and BChE ($K_i = 20.41 \mu$ M), therefore suggesting that it may be capable of binding to the peripheral anionic site (PAS) and catalytic anionic site (CAS) of both enzymes. Kinetic studies

were also performed for compounds **9a**, **5b** and **10b** and a mixed-type inhibition mechanism for both enzymes was also established for the three compounds (supporting information Figures S46–S48).

It has been shown that AChE promotes amyloid fibril formation by interaction through the PAS giving stable AChE– $A\beta$ complexes, which are more toxic than single $A\beta$ peptides (Reyes et al., 2004). Dual-site inhibitors, which can interact with both the CAS and PAS, could not only restore cholinergic transmission, but also inhibit the production or the aggregation of $A\beta$ promoted by AChE (Fernández-Bachiller et al., 2012; Özturan Özer et al., 2013). Therefore, dual-site inhibitors may contribute significantly to delay the progression of AD and emerge as promising drug candidates for the treatment of AD.

Prediction of blood–brain barrier (BBB) permeability

The following parameters associated with solubility and permeability for imine **9a** and amines **3b**, **5b–11b** were predicted by using SwissADME server (<http://www.swissadme.ch/index.php>; Daina et al., 2017) and are gathered in Table 2: average of predictions of theoretical octanol/water partition coefficients (Log P), molecular weight (MW), the number of H-bond donors (HBD—expressed as the sum of OHs and NHs) and the number of acceptors (HBA—the sum of Ns and Os). Lipinski's rule of five for CNS penetration, used to predict the suitability of orally administered drug candidates, states that CNS penetration is likely if $MW < 400$, $HBD \leq 3$, $HBA \leq 7$ and $\text{Log } p \leq 5$ (Pajouhesh & Lenz, 2005). The results indicate that all compounds, with the exception of Br-substituted **7b** and **10b**, satisfy the criteria of the Lipinski's rule of 5 for CNS and are BBB permeable.

Docking studies

The best redocking results presented random mean square deviation (RMSD) values of 1.19 and 0.53 Å for *Ee*AChE and *Eq*BChE, respectively. This is enough to validate our docking protocol once the literature considers a RMSD value below 2.50 Å as acceptable for this purpose (Kontoyianni et al., 2004). The protein–ligand interaction energies were calculated in order to compare the best poses obtained for each compound and also to verify the residues contributing for the stabilization of each ligand inside the enzymes. Furthermore, the dockings were expected to provide insight into molecular recognition for the cholinesterase inhibition assays. The results are gathered in Table 3.

Results from the Chemicalize server (<https://chemicalize.com/>) showed that the most prevalent chemical species of the ligands should be positively charged at pH 7.4, bearing the NH close to the protonated phenolic ring. The only exception was amine **9a**, for which the most prevalent species at pH 7.4 pointed by the server (<https://chemicalize.com/>) is the neutral molecule. The docking studies are in agreement with the experimental results that evidenced selectivity towards *Ee*AChE, since all compounds presented lower values of intermolecular energy inside *Ee*AChE

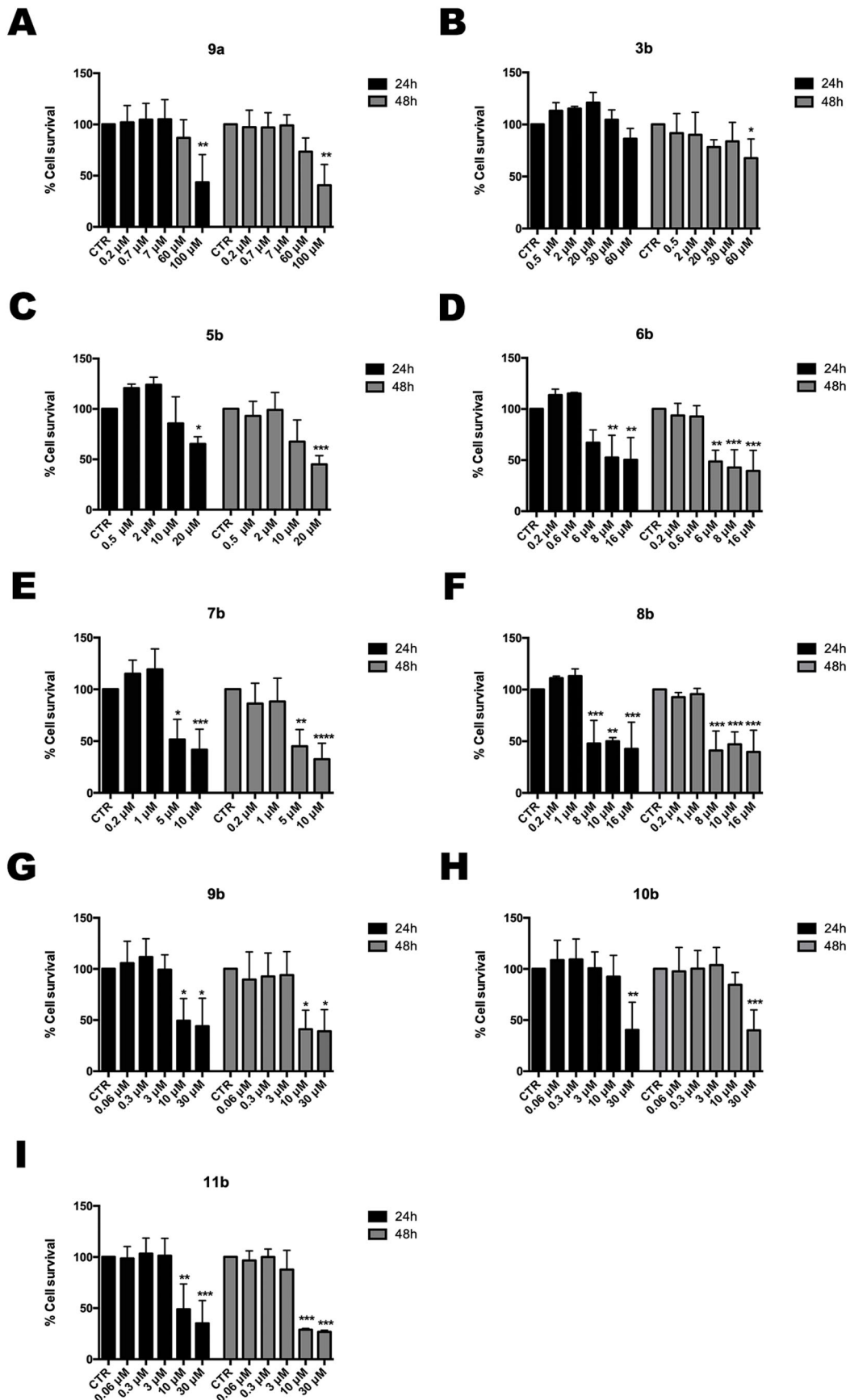


Figure 1. Viability of astrocytes under incubation for 24 and 48 h (MTT Assay) with **9a** (a), **3b** (b), **5b** (c), **6b** (d), **7b** (e), **8b** (f), **9b** (g), **10b** (h), **11b** (i). The results present the average values \pm standard deviation from three experiments in triplicate. **** $p < 0.0001$ relative to control (CTR).

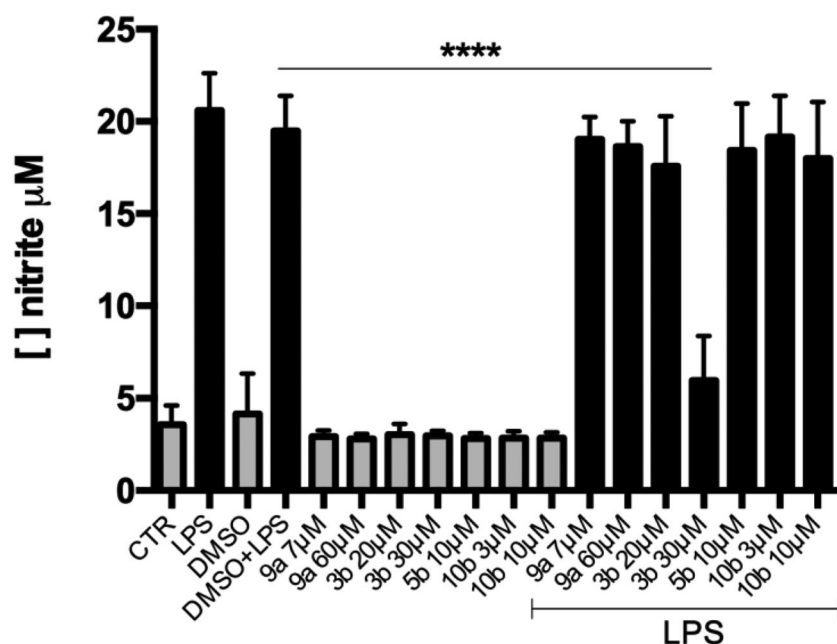


Figure 2. The compounds did not induce $\text{NO}\bullet$ secretion by N9 microglial lineage cells. N9 cells were incubated for 48 h in the presence of DMEM-F12 without serum (control = CTR). LPS ($1 \mu\text{g}\cdot\text{mL}^{-1}$) was used as positive control. Compound concentrations were based on the IC_{50} values for AChE and BChE. The culture medium of each sample was collected for further analysis of $\text{NO}\bullet$ production (Griess reaction). The results present the average values \pm standard deviation from three experiments in triplicate. Note that 3b reduced the release of $\text{NO}\bullet$ at $30 \mu\text{M}$ + LPS. **** $p < 0.0001$ relative to control (dimethyl sulfoxide (DMSO) + LPS).

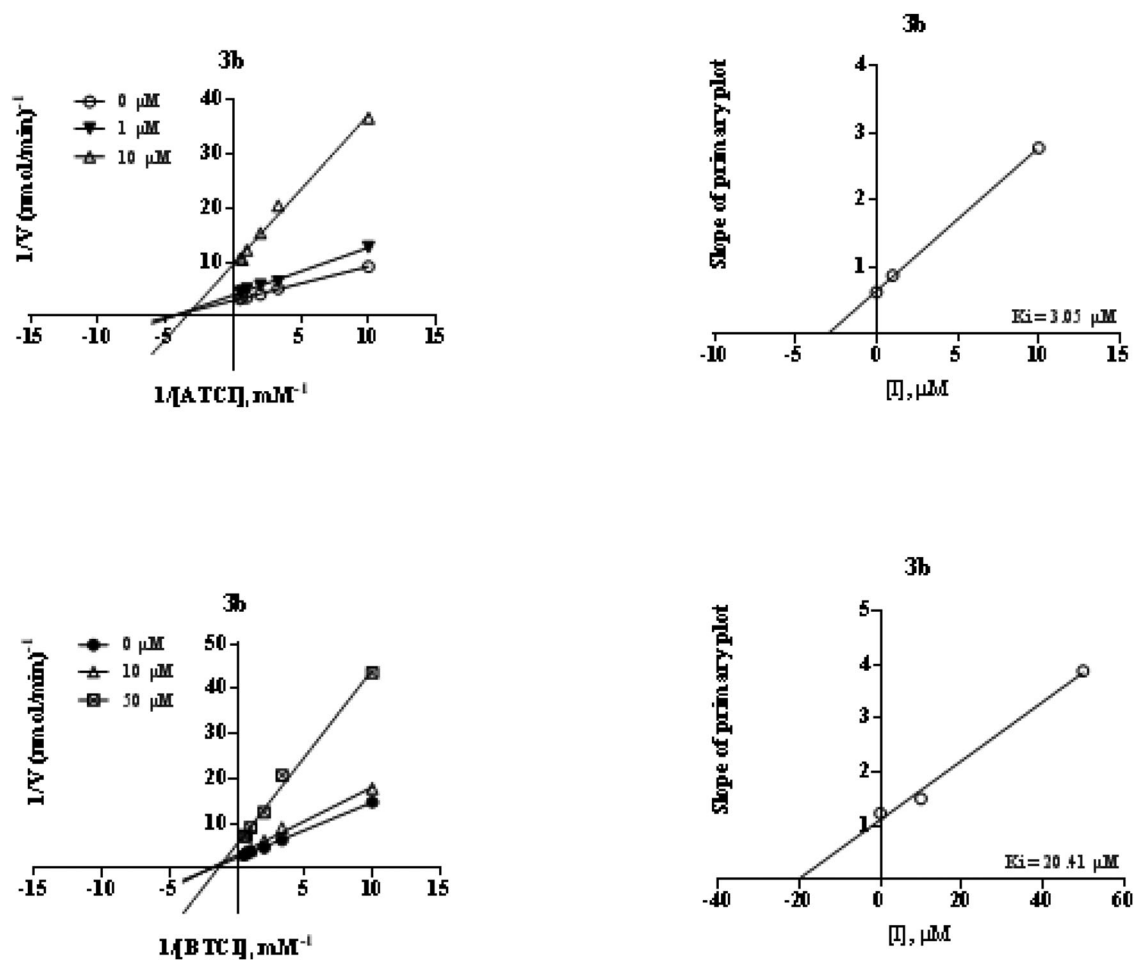


Figure 3. Kinetic study of the mechanisms of EeAChE (top) and EqBChE (bottom) inhibition by compound 3b. (Left) Lineweaver–Burk reciprocal plots of the cholinesterase initial velocity at increasing substrate concentrations. (Right) Secondary plot of slope (K_m/V_{max}) versus compound concentration.

compared to *EqBChE* (see Table 3). We suppose that the ligands fit better inside the smaller cavity of *EeAChE* (149.50 Å³) than in the almost three times larger cavity of *EqBChE* (414.72 Å³), whose volumes were calculated by using MVD® (Thomsen & Christensen, 2006). In the latter, appropriate anchoring and further binding to the active sites are probably less effective than in the *EeAChE* cavity, reflecting in less negative energy values.

As illustrated in Figures 4, S49, and S50, the best poses of compounds **9a**, **3b** and **9b** show interactions with the residues belonging to several sub-sites of the active site gorges of *EeAChE* and *EqBChE* (Nuthakki et al., 2019), including PAS and CAS. This is in line with the aforementioned experimental data that indicated mixed type inhibition of these compounds towards both AChE and BChE.

For imine **9a** (see supporting information Figures S49(a,b)) H-bonds were observed with Gly120 (oxyanion hole) and Tyr337 (anionic sub-site) of AChE, and with Ser79 and His438 (CAS) of BChE, whereas π - π interactions were observed with Trp86, which is the key residue of the anionic subsite of AChE, and with Trp82 (anionic site) of BChE. Besides, the quinoline ring of **9a** docked close to the AChE aromatic residues Tyr124 (PAS), Phe295 and Phe297 (acyl binding pocket), Tyr341 (PAS) and Phe338 (anionic subsite), and between residues Trp82 (anionic site) and His438 (CAS) of BChE.

Amine **3b** (see Figure 4(a,b)) established H-bonds with residues Gly120 (oxyanion hole) and Tyr124 (PAS) of AChE, and Ser198 and His438 (both from CAS) of BChE. This

compound also established π - π interactions with Trp82 (anionic sub-site) and Trp286 (PAS) of AChE, and with Trp82 (anionic site) of BChE. The quinoline ring of **3b** accommodated among the aromatic residues Trp286 (PAS), Phe295 and Phe297 (both from the acyl binding pocket) and Tyr337 and Phe338 (anionic sub-site) of AChE, and Trp82 (anionic site) and His438 (CAS) of BChE.

Compound **9b** (see supporting information Figures S50(a,b)) established H-bonds with Gly120 (oxyanion hole) of AChE and Leu286 of BChE (acyl binding pocket). π - π stacking interactions were observed with Trp286 (PAS) of AChE, and Trp82 (anionic site) of BChE. The quinoline ring of this compound accommodated among residues Tyr124 and Trp286 (both from PAS), and Phe297 (acyl binding pocket) of AChE, whereas inside BChE, it appears between residues Trp82 (anionic site) and His438 (CAS), with the phenolic ring between residues Trp231 and Phe329 (anionic site).

Conclusion

In this work, a series of 7-chloro-4-aminoquinoline derivatives containing methylene spacers of different sizes between the 7-chloro-4-aminoquinoline nucleus and imino methyl substituted phenolic rings (imines **6a–11a**) and their reduced analogues (amines **3b–11b**) were investigated as multifunctional cholinesterase inhibitors. Compounds **9a**, **3b**, **5b** and **10b** inhibited both cholinesterases, being more selective for AChE. Both the reduction of the double bond and the increase of the alkyl chain have been shown to contribute to the increase of the inhibitory potency of the compounds. Kinetic and molecular modeling studies indicated that these compounds show mixed-type inhibition of both enzymes, binding simultaneously to the active and peripheral sites therein. They were non-cytotoxic and did not stimulate pro-inflammatory activity in glial cells. Interestingly, while the remaining compounds were unable to prevent the inflammatory response stimulated by LPS, compound **3b** (30 μ M) showed promising anti-inflammatory activity by reducing the microglial release of NO• at a concentration that is equivalent to the IC₅₀ of BChE and 15-fold greater than the AChE IC₅₀. Nitric oxide secretion is one of the neurotoxic and pro-inflammatory factors attributed to

Table 2. Molecular descriptors of compounds **9a**, **3b**, **5b–11b**, tacrine, donepezil and galantamine.

Compound	MW	LogP	HBD	HBA
9a	381.90	4.72	2	3
3b	327.81	3.28	3	3
5b	341.83	3.66	3	3
6b	355.86	3.94	3	3
7b	434.76	4.58	3	3
8b	369.89	4.23	3	3
9b	397.94	4.56	3	3
10b	462.81	5.18	3	3
11b	397.94	4.91	3	3
Tacrine	197.28	2.59	1	1
Donepezil	379.49	4.00	0	4
Galantamine	287.35	1.91	1	4

Table 3. Docking results.

Ligand	<i>EeAChE</i>			<i>EqBChE</i>		
	Energy (kcal.mol ⁻¹)	H-bond interactions	E _{H-bond} (kcal.mol ⁻¹)	Energy (kcal.mol ⁻¹)	H-bond interactions	E _{H-bond} (kcal.mol ⁻¹)
Donepezil(<i>EeAChE</i>)	-96.38	Tyr124	-2.50	-89.65	-	0.00
Tacrine (<i>EqBChE</i>)						
9a	-159.21	Gly120 Tyr337	-1.76	-125.64	Asp70 Ser79 His438	-5.45
3b	-153.73	Gly120 Tyr124	-5.00	-129.64	Ser198 His438	-1.70
5b	-153.02	Gly120 Tyr124	-4.02	-136.57	Asn68 Asp70(2×) Ser79 Asn83 Tyr332	-6.36
6b	-162.07	Gly120 Tyr337	-2.11	-137.90	Ser287 His438	-1.62
7b	-158.22	Gly120 Tyr124	-2.72	-142.13	Asp70 Ser287	-2.46
8b	-157.59	Gly120 Tyr124 Tyr337	-7.16	-138.01	Ser287 His438	-2.77
9b	-163.13	Gly120	-2.50	-139.91	Leu286	-0.07
10b	-164.76	Gly120 Tyr124	-2.89	-149.63	Asp70 Tyr332 His438	-1.75
11b	-164.95	Gly120	-1.76	-152.84	Ser198(3×) Tyr332	-4.83

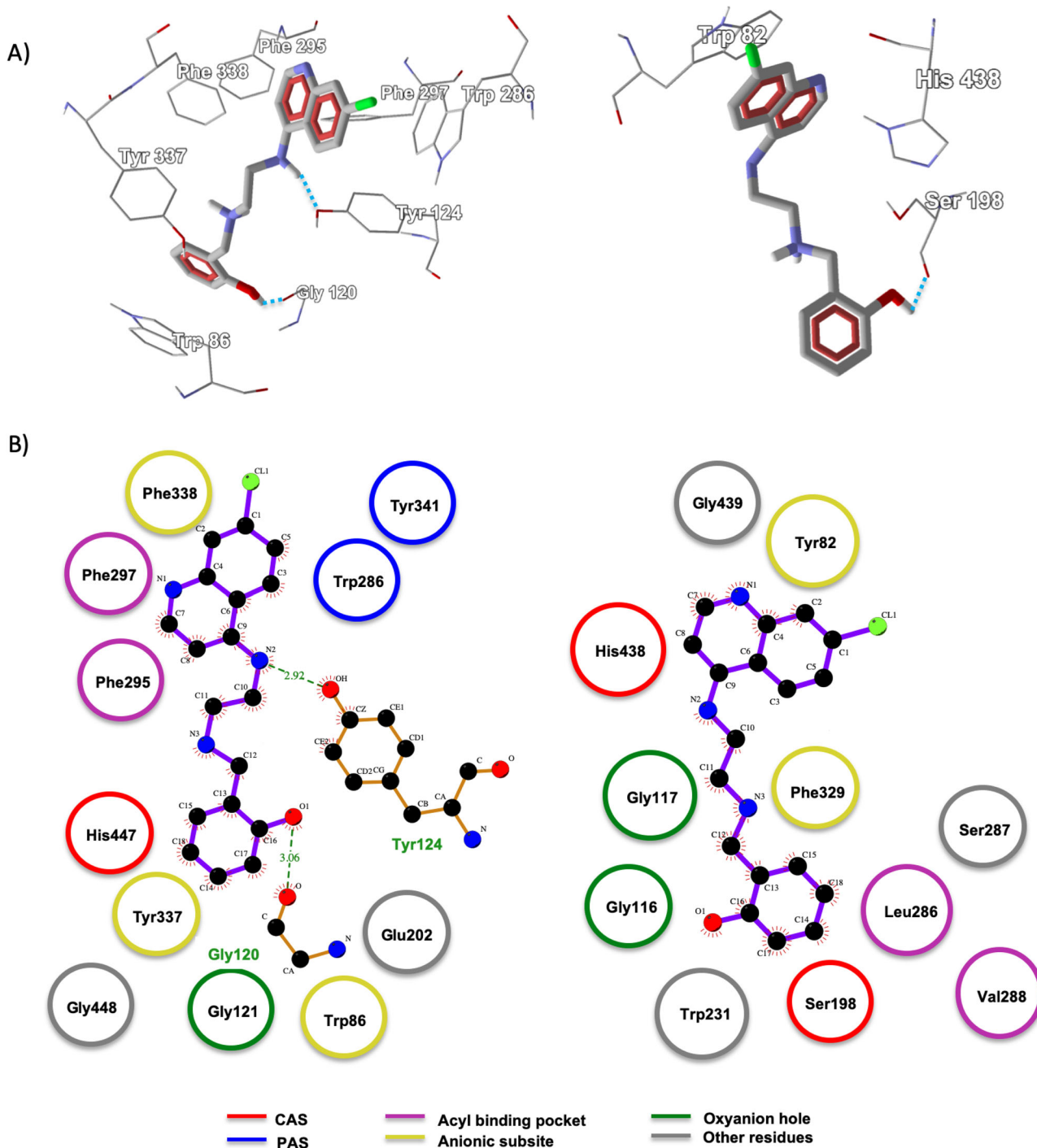


Figure 4. (a) Selected interactions of the best poses of **3b** inside EeAChE (left) and EqBChE (right). H-bonds are shown in blue dotted lines. (b) Interactions of the best poses of **3b** inside EeAChE (left) and EqBChE (right).

inflammation-mediated neurodegeneration (Wyss-Coray & Mucke, 2002). In *in silico* calculations **3b** showed the best ability to cross BBB. Taken together, **3b** emerges as a possible prototype with multi-target actions, as a dual-site inhibitor of AChE and anti-neuroinflammatory, and can be very useful in the prevention of neurodegeneration. In addition, imine **9a** and amines **3b**, **5b** and **10b** are potent dual-site inhibitors of AChE and have high potential for being evaluated in other targets of AD, such as beta amyloid, tau protein and also on neuronal nicotinic acetylcholine receptor alpha7 ($\alpha 7nAChR$).

Experimental

Chemistry

4,7-Dichloroquinoline (97%), ethane-1,2-diamine (99%), 1,4-diaminobutane (99%), 1,6-hexanediamine (98%), 5-bromo-2-hydroxybenzaldehyde (98%), 2-hydroxy-5-methylbenzaldehyde (98%), sodium borohydride (98%) were purchased from Sigma-Aldrich and 2-hydroxybenzaldehyde, from Merck (>99%). All other reagents were purchased from Sigma-Aldrich or Vetec chemicals and were used without further purification. The precursors *N*-(7-chloro-4-quinolyl)-1,4-

diaminobutane (**1**) and *N*-(7-chloro-4-quinolyl)-1,6-diaminohexane (**2**) were prepared as described in the literature and its identity and purity were confirmed by mp, IR and ^1H NMR spectroscopy (Natarajan et al., 2008). Schiff bases (*E*)-2-((2-(7-chloroquinolin-4-ylamino)ethylimino) methyl)phenol (**3a**), (*E*)-4-bromo-2-((2-(7-chloroquinolin-4-ylamino)ethylimino)methyl)phenol (**4a**) and (*E*)-2-((2-(7-chloroquinolin-4-ylamino)ethylimino)methyl)-4-methylphenol (**5a**) were previously synthesized (Zanon et al., 2019).

CHN elemental analyses were carried out using a Perkin-Elmer 2400 at Universidade de São Paulo (USP-SP), Brazil. NMR spectra were recorded on a Varian VNMRS (^1H at 300 or 500 MHz, ^{13}C NMR 125 or 75 MHz) spectrometer with dimethyl sulfoxide- d_6 (DMSO- d_6) or chloroform- d (CDCl_3) as the solvent. FTIR spectra were measured using a Varian 600 FTIR spectrometer equipped with a Pike ATR Miracle accessory (diamond/ZnSe crystal, resolution: 4 cm^{-1}) at room temperature in the range between 4000 and 600 cm^{-1} with 32 scans.

General method for the synthesis of imines

Salicylaldehydes were stirred overnight with **1** in ethanol, at room temperature, whereas their reactions with **2** were stirred at 50°C for 3 h, and then kept at room temperature also overnight. In the absence of a precipitate, the solvent was removed under reduced pressure yielding the product. The compounds were washed with diethyl ether.

(*E*)-2-(((4-((7-Chloroquinolin-4-yl)amino)butyl)imino)methyl)phenol, **6a**

The yellow powder **6a** was obtained from 2-hydroxybenzaldehyde (0.73 μL , 0.70 mmol) and **1** (125 mg, 0.50 mmol). Yield: 79% (140 mg). Mp: 165°C . Elemental analysis (%) calcd. for $\text{C}_{20}\text{H}_{20}\text{ClN}_3\text{O}$: C 67.89, H 5.70, N 11.88, found: C 67.57, H 5.65, N 11.75. ^1H NMR (300 MHz, CDCl_3): δ 13.46 (OH), 8.52 (1H, d, $J=5.3$ Hz), 8.37 (1H, s), 7.95 (1H, d, $J=2.1$ Hz), 7.64 (1H, d, $J=8.9$ Hz), 7.35–7.29 (2H, m), 7.25 (1H, m), 6.65 (1H, dd, $J=7.5, 0.6$ Hz), 6.89 (1H, td, $J=7.5, 1.0$ Hz), 6.41 (1H, d, $J=5.3$ Hz), 4.98 (1H, NH), 3.68 (2H, m), 3.37 (2H, m), 1.88 (4H, m). ^{13}C NMR (125 MHz, DMSO- d_6): δ 166.2, 161.3, 152.3, 150.5, 149.6, 133.8, 132.6, 132.0, 127.9, 124.5, 124.4, 119.1, 118.8, 117.9, 116.9, 99.1, 58.4, 42.6, 28.4, 25.9. IR (ATR, $\nu_{\text{max}}/\text{cm}^{-1}$): 3329, 2954, 2883, 1633 (C=N imine), 1610 (7-chloroquinoline), 1581 (7-chloroquinoline), 1537 (7-chloroquinoline), 1489, 1456, 1375, 1333, 1290, 1198, 1155, 1076, 1026, 895, 868, 812, 760, 738.

(*E*)-4-Bromo-2-(((4-((7-chloroquinolin-4-yl)amino)butyl)imino)methyl)phenol, **7a**

The yellow powder **7a** was obtained from 5-bromo-2-hydroxybenzaldehyde (190 mg, 0.95 mmol) and **1** (187 mg, 0.75 mmol). Yield: 71% (307 mg). Mp: 182°C . Elemental analysis (%) calcd. for $\text{C}_{20}\text{H}_{19}\text{BrClN}_3\text{O}$ ·0.3/5 diethyl ether: C 54.55, H 4.71, N 9.36, found: C 54.99, H 4.30, N 9.14. ^1H NMR (500 MHz, CDCl_3): δ 13.45 (OH), 8.53 (1H, d, $J=5.2$ Hz), 8.29 (1H, s), 7.96 (1H, d, $J=2.1$ Hz), 7.64 (1H, d, $J=8.9$ Hz), 7.39

(1H, dd, $J=8.7, 2.4$ Hz), 7.36 (2H, m), 6.86 (1H, d, $J=8.7$ Hz), 6.41 (1H, d, $J=5.2$ Hz), 4.96 (1H, NH), 3.69 (2H, m), 3.37 (2H, m), 1.85 (4H, m). ^{13}C NMR (125 MHz, DMSO- d_6): δ 165.0, 161.2, 152.3, 150.6, 149.6, 135.1, 133.8, 133.8, 128.0, 124.5, 124.4, 120.7, 119.6, 118.0, 109.2, 99.2, 58.0, 42.6, 28.3, 26.0. IR (ATR, $\nu_{\text{max}}/\text{cm}^{-1}$): 3209 (N-H), 3061, 2957, 2870, 1637 (C=N imine), 1610 (7-chloroquinoline), 1577 (7-chloroquinoline), 1550 (7-chloroquinoline), 1479, 1450, 1428, 1365, 1333, 1278, 1205, 1137, 1080, 1035, 895, 865, 848, 808, 766, 690, 642, 624.

(*E*)-2-(((4-((7-Chloroquinolin-4-yl)amino)butyl)imino)methyl)-4-methylphenol, **8a**

The yellow powder **8a** was obtained from 2-hydroxy-5-methylbenzaldehyde (95.2 mg, 0.70 mmol) and **1** (125 mg, 0.50 mmol). Yield: 79% (145 mg). mp: 176°C . Elemental analysis (%) calcd. for $\text{C}_{21}\text{H}_{22}\text{ClN}_3\text{O}$: C 68.56, H 6.03, N 11.42; found: C 68.84, H 6.04, N 11.32. ^1H NMR (300 MHz, CDCl_3): δ 13.19 (OH), 8.51 (1H, d, $J=5.3$ Hz), 8.32 (1H, s), 7.95 (1H, d, $J=2.1$ Hz), 7.64 (1H, d, $J=8.9$ Hz), 7.34 (1H, dd, $J=8.9, 2.1$ Hz), 7.13 (1H, dd, $J=8.4, 2.1$ Hz), 7.03 (1H, d, $J=2.1$ Hz), 6.87 (1H, d, $J=8.4$ Hz), 6.40 (1H, d, $J=5.3$ Hz), 4.99 (1H, NH), 3.67 (2H, m), 3.36 (2H, m), 2.29 (3H, s), 1.87 (4H, m). ^{13}C NMR (125 MHz, DMSO- d_6): δ 166.4, 158.8, 152.3, 150.5, 149.6, 133.8, 133.3, 131.8, 127.9, 127.4, 124.5, 124.4, 118.8, 117.9, 116.7, 99.6, 58.6, 42.6, 28.5, 25.9, 20.3. IR (ATR, $\nu_{\text{max}}/\text{cm}^{-1}$): 3389, 3242 (N-H), 3059, 2932, 2853, 1633 (C=N imine), 1610 (7-chloroquinoline), 1581 (7-chloroquinoline), 1538 (7-chloroquinoline), 1498, 1450, 1369, 1354, 1330, 1284, 1242, 1159, 1139, 1078, 1405, 886, 868, 843, 808, 785, 640.

(*E*)-2-(((6-((7-Chloroquinolin-4-yl)amino)hexyl)imino)methyl)phenol, **9a**

The yellow powder **9a** was obtained from 2-hydroxybenzaldehyde (100 μL , 1.00 mmol) and **2** (278 mg, 1.00 mmol). Yield: 82% (313 mg). mp: 113°C . Elemental analysis (%) calcd. For $\text{C}_{22}\text{H}_{24}\text{ClN}_3\text{O}$: C 69.19, H 6.33, N 11.00; found: C 68.73, H 6.15, N 10.60. ^1H NMR (500 MHz, DMSO- d_6): δ 13.66 (OH), 8.53 (1H, s), 8.36 (1H, d, $J=5.4$ Hz), 8.26 (1H, d, $J=9.0$ Hz), 7.76 (1H, d, $J=2.2$ Hz), 7.40 (2H, td, $J=9.0, 2.2$ Hz), 7.31 (1H, m), 7.25 (1H, NH), 6.87 (2H, m), 6.44 (1H, d, $J=5.4$ Hz), 3.59 (2H, t), 3.25 (2H, m), 1.67 (4H, m), 1.42 (4H, m). ^{13}C NMR (75 MHz, DMSO- d_6): δ 166.2, 161.5, 152.3, 150.7, 149.7, 133.8, 132.6, 131.9, 128.0, 124.5, 124.3, 119.1, 118.7, 118.0, 117.0, 99.4, 58.5, 42.9, 30.7, 28.3, 26.8, 26.8. IR (ATR, $\nu_{\text{max}}/\text{cm}^{-1}$): 3230 (N-H), 3062, 2933, 2860, 1635 (C=N imine), 1611 (7-chloroquinoline), 1577 (7-chloroquinoline), 1544 (7-chloroquinoline), 1452, 1426, 1365, 1335, 1321, 1281, 1226, 1200, 1134, 1080, 1038, 978, 960, 895, 865, 847, 798, 754, 732, 636.

(*E*)-4-bromo-2-(((6-((7-chloroquinolin-4-yl)amino)hexyl)imino)methyl)phenol, **10a**

The yellow powder **10a** was obtained from 5-bromo-2-hydroxybenzaldehyde (200 mg, 1.00 mmol) and **2** (278 mg, 1.00 mmol). Yield: 81% (372 mg). mp: 126°C . Elemental analysis (%) calcd. for $\text{C}_{22}\text{H}_{23}\text{BrClN}_3\text{O}$: C 57.34, H 5.03, N 9.12;

found: C 57.31, H 5.18, N 9.12. ^1H NMR (500 MHz, DMSO- d_6) δ 13.83 (OH), 8.52 (1H, s), 8.37 (1H, d, $J=5.4$ Hz), 8.26 (1H, d, $J=9.0$ Hz), 7.76 (1H, d, $J=2.2$ Hz), 7.62 (1H, d, $J=2.5$ Hz), 7.44 (2H, m), 7.24 (1H, NH), 6.82 (1H, d, $J=8.8$ Hz), 6.44 (1H, d, $J=5.4$ Hz), 3.60 (2H, t), 3.22 (2H, m), 1.67 (4H, m), 1.42 (4H, m). ^{13}C NMR (125 MHz, DMSO- d_6): δ 164.8, 161.2, 152.3, 150.6, 149.6, 135.1, 133.8, 128.0, 124.5, 124.3, 120.7, 119.7, 118.0, 109.2, 99.1, 58.2, 42.9, 30.6, 28.3, 26.8, 26.7. IR (ATR, $\nu_{\text{max}}/\text{cm}^{-1}$): 3230 (N-H), 3064, 2935, 2856, 1631 (C=N imine), 1612 (7-chloroquinoline), 1579 (7-chloroquinoline), 1547 (7-chloroquinoline), 1477, 1453, 1430, 1365, 1332, 1320, 1281, 1200, 1136, 1080, 1016, 960, 898, 866, 812, 765, 698, 642, 625.

(E)-2-(((6-((7-Chloroquinolin-4-yl)amino)hexyl)imino)methyl)-4-methylphenol, 11a

The yellow powder **11a** was obtained from 2-hydroxy-5-methylbenzaldehyde (163 mg, 1.20 mmol) and **2** (278 mg, 1.00 mmol). Yield: 36% (140 mg). mp: 108 °C. Elemental analysis (%) calcd. for $\text{C}_{23}\text{H}_{26}\text{ClN}_3\text{O}\cdot 1/3\text{H}_2\text{O}$: C 68.73, H 6.69, N 10.45; found: C 68.99, H 6.43, N 10.46. ^1H NMR (500 MHz, DMSO- d_6): δ 13.31 (OH), 8.46 (1H, s), 8.37 (1H, d, $J=5.4$ Hz), 8.26 (1H, d, $J=9.0$ Hz), 7.76 (1H, d, $J=2.2$ Hz), 7.42 (1H, dd, $J=9.0, 2.2$ Hz), 7.23 (1H, NH), 7.19 (1H, d, $J=1.9$ Hz), 7.12 (1H, dd, $J=8.3, 1.9$ Hz), 6.76 (1H, d, $J=8.3$ Hz), 6.44 (1H, d, 5.4 Hz), 3.58 (2H, t), 3.25 (2H, m), 2.23 (3H, s), 1.66 (4H, m), 1.42 (4H, m). ^{13}C NMR (75 MHz, DMSO- d_6): δ 165.2, 158.4, 151.7, 150.0, 149.0, 133.2, 132.7, 131.2, 127.3, 126.8, 123.9, 123.8, 118.2, 117.4, 116.1, 98.8, 58.2, 42.3, 30.2, 27.6, 26.2, 26.2, 19.8. IR (ATR, $\nu_{\text{max}}/\text{cm}^{-1}$): 3251 (N-H), 3062, 2933, 2854, 1635 (C=N imine), 1612 (7-chloroquinoline), 1577 (7-chloroquinoline), 1549 (7-chloroquinoline), 1468, 1493, 1427, 1363, 1334, 1319, 1281, 1255, 1198, 1142, 1080, 1039, 1016, 957, 899, 865, 847, 806, 796, 781, 763, 732, 672, 635.

General method for the reduction of the imines

To an ice-cold solution of the Schiff base in ethanol NaBH_4 was added in portions. The reaction was followed by thin layer chromatography (TLC) using CH_2Cl_2 /methanol 1:1 as eluent. After complete disappearance of the starting material, the reaction mixture was quenched by careful addition of HCl (6 mol.L $^{-1}$) until pH 1. The solvent was removed under reduced pressure and water was added (20–40 mL). The resulting aqueous solution was basified with NaOH (4 mol.L $^{-1}$) until pH 10, and then extracted with CH_2Cl_2 . The organic layer was dried over anhydrous MgSO_4 , filtered and concentrated under reduced pressure to yield the products as white powders.

2-(((2-((7-Chloroquinolin-4-yl)amino)ethyl)amino)methyl)phenol, 3b

3b was obtained from **3a** (162 mg, 0.50 mmol) and NaBH_4 (26.4 mg, 0.70 mmol). Yield: 76% (125 mg). mp: 146 °C. Elemental analysis (%) calcd. for $\text{C}_{18}\text{H}_{18}\text{ClN}_3\text{O}\cdot 1/4\text{H}_2\text{O}$: C 65.06, H 5.61, N 12.64; found: C 65.28, H 5.38, N 12.51. ^1H NMR (500 MHz, CDCl_3): δ 8.52 (1H, d, $J=5.4$ Hz), 7.95 (1H, d,

$J=2.1$ Hz), 7.75 (1H, d, $J=8.9$ Hz), 7.40 (1H, dd, $J=8.9, 2.1$ Hz), 7.20 (1H, td, $J=8.0, 1.0$ Hz), 7.02 (1H, dd, $J=7.4, 0.8$ Hz), 6.88 (1H, dd, $J=8.0, 0.8$ Hz), 6.82 (1H, td, $J=7.4, 1.0$ Hz), 6.38 (1H, d, $J=5.4$ Hz), 5.30 (1H, NH), 4.10 (2H, s), 3.47 (2H, m), 3.07 (2H, m). ^{13}C NMR (75 MHz, DMSO- d_6): δ 157.5, 152.3, 150.6, 149.5, 133.8, 129.1, 128.3, 127.9, 124.8, 124.5, 124.5, 119.0, 118.0, 115.8, 99.2, 50.4, 46.8, 42.6. IR (ATR, $\nu_{\text{max}}/\text{cm}^{-1}$): 3307, 3189 (N-H), 3043, 2931, 2843, 2698, 2559, 1610 (7-chloroquinoline), 1579 (7-chloroquinoline), 1547 (7-chloroquinoline), 1492, 1446, 1426, 1371, 1348, 1331, 1269, 1250, 1231, 1196, 1134, 1099, 1082, 1036, 968, 906, 868, 814, 804, 780, 750, 730, 681, 618.

4-Bromo-2-(((2-((7-chloroquinolin-4-yl)amino)ethyl)amino)methyl)phenol, 4b

4b was obtained from **4a** (121 mg, 0.30 mmol) and NaBH_4 (19.0 mg, 0.50 mmol). Yield: 67% (82.5 mg). mp: 167 °C. Elemental analysis (%) calcd. for $\text{C}_{18}\text{H}_{17}\text{BrClN}_3\text{O}\cdot 1/3\text{CH}_2\text{Cl}_2$: C 50.62, H 4.09, N 9.66; found: C 50.34, H 4.28, N 9.51. ^1H NMR (500 MHz, CDCl_3): δ 8.45 (1H, d, $J=5.3$ Hz), 7.88 (1H, d, $J=2.1$ Hz), 7.65 (1H, d, $J=8.9$ Hz), 7.34 (1H, dd, $J=8.9, 2.1$ Hz), 7.21 (1H, dd, $J=8.6, 2.4$ Hz), 7.07 (1H, d, $J=2.4$ Hz), 6.68 (1H, d, $J=8.6$ Hz), 6.32 (1H, d, $J=5.3$ Hz), 5.18 (1H, NH), 3.98 (2H, s), 3.42 (2H, m), 2.99 (2H, m). ^{13}C NMR (75 MHz, DMSO- d_6): δ 156.6, 152.3, 150.6, 149.7, 133.8, 131.5, 130.6, 128.2, 128.0, 124.4, 124.3, 118.0, 117.9, 110.2, 99.2, 49.4, 47.0, 42.7. IR (ATR, $\nu_{\text{max}}/\text{cm}^{-1}$): 3215 (N-H), 3014, 2940, 2845, 2771, 1610 (7-chloroquinoline), 1581 (7-chloroquinoline), 1557 (7-chloroquinoline), 1534, 1496, 1448, 1427, 1385, 1372, 1345, 1329, 1275, 1233, 1215, 1196, 1175, 1134, 1086, 1039, 1019, 997, 974, 906, 870, 843, 806, 769, 659, 621.

2-(((2-((7-Chloroquinolin-4-yl)amino)ethyl)amino)methyl)-4-methylphenol, 5b

5b was obtained from **5a** (170 mg, 0.50 mmol) and NaBH_4 (26.4 mg, 0.70 mmol). Yield: 76% (129 mg). mp: 154 °C. Elemental analysis (%) calcd. for $\text{C}_{19}\text{H}_{20}\text{ClN}_3\text{O}$: C 66.67, H 5.90, N 12.29; found: C 66.47, H 5.75, N 12.01. ^1H NMR (500 MHz, CDCl_3): δ 8.50 (1H, d, $J=5.3$ Hz), 7.94 (1H, d, $J=2.1$ Hz), 7.74 (1H, d, $J=8.9$ Hz), 7.38 (1H, dd, $J=8.9, 2.1$ Hz), 6.99 (1H, dd, $J=8.1, 1.7$ Hz), 6.82 (1H, d, $J=1.7$ Hz), 6.78 (1H, d, $J=8.1$ Hz), 6.36 (1H, d, $J=5.3$ Hz), 5.34 (1H, NH), 4.05 (2H, s), 3.45 (2H, m), 3.05 (2H, m), 2.24 (3H, s). ^{13}C NMR (125 MHz, DMSO- d_6): δ 155.1, 152.3, 150.6, 149.5, 133.8, 129.6, 128.5, 127.9, 127.3, 124.5, 124.5, 118.0, 115.6, 99.1, 50.4, 46.7, 42.6, 20.5. IR (ATR, $\nu_{\text{max}}/\text{cm}^{-1}$): 3303, 3198 (N-H), 2914, 2846, 2569, 1610 (7-chloroquinoline), 1583 (7-chloroquinoline), 1548 (7-chloroquinoline), 1510, 1495, 1446, 1429, 1385, 1373, 1344, 1333, 1263, 1234, 1211, 1194, 1136, 1099, 1084, 1034, 964, 920, 901, 872, 810, 777, 683, 654, 638, 620.

2-(((4-((7-Chloroquinolin-4-yl)amino)butyl)amino)methyl)phenol, 6b

6b was obtained from **6a** (88.5 mg, 0.25 mmol) and NaBH_4 (17.0 mg, 0.45 mmol). Yield: 78% (70 mg). mp: 109 °C. Elemental analysis (%) calcd. for $\text{C}_{20}\text{H}_{22}\text{ClN}_3\text{O}\cdot 1/3\text{H}_2\text{O}$: C

66.38, H 6.31, N 11.61; found: C 66.38, H 6.07, N 11.22. ^1H NMR (500 MHz, CDCl_3): δ 8.46 (1H, d, $J=5.3$ Hz), 7.89 (1H, d, $J=2.1$ Hz), 7.59 (1H, d, $J=8.9$ Hz), 7.29 (1H, dd, $J=8.9$, 2.1 Hz), 7.11 (1H, td, $J=8.0$, 1.7 Hz), 6.92 (1H, dd, $J=7.4$, 1.7 Hz), 6.77 (1H, dd, $J=8.0$, 1.1 Hz), 6.72 (1H, td, $J=7.4$, 1.1 Hz), 6.32 (1H, d, $J=5.3$ Hz), 4.96 (s, NH), 3.95 (2H, s), 3.28–3.24 (2H, dd, $J=6.9$ Hz), 2.70 (2H, t, $J=6.9$ Hz), 1.80–1.73 (2H, m), 1.64 (2H, m). ^{13}C NMR (125 MHz, $\text{DMSO}-d_6$): δ 157.2, 151.6, 149.9, 148.9, 133.1, 128.2, 127.5, 127.2, 123.9, 123.7, 123.6, 118.1, 117.3, 115.1, 98.6, 50.5, 47.7, 42.1, 26.4, 25.5. IR (ATR, $\nu_{\text{max}}/\text{cm}^{-1}$): 3281, 3241, 3061, 2958, 1611 (7-chloroquinoline), 1578 (7-chloroquinoline), 1565 (7-chloroquinoline), 1550 (7-chloroquinoline), 1492, 1477, 1467, 1451, 1426, 1379, 1361, 1338, 1320, 1280, 1248, 1216, 1207, 1145, 1105, 929, 894, 863, 847, 759, 749, 716, 629.

4-Bromo-2-(((4-((7-chloroquinolin-4-yl)amino)butyl)amino)methyl)phenol, 7b

7b was obtained from **7a** (130 mg, 0.30 mmol) and NaBH_4 (19.0 mg, 0.50 mmol). Yield: 42% (55 mg). mp: 126 °C. Elemental analysis (%) calcd. for $\text{C}_{20}\text{H}_{21}\text{BrClN}_3\text{O}_1/7\text{H}_2\text{O}$: C 54.93, H 4.91, N 9.61; found: C 55.37, H 4.76, N 9.19. ^1H NMR (500 MHz, CDCl_3): δ 8.53 (1H, d, $J=5.3$ Hz), 7.96 (1H, d, $J=2.1$ Hz), 7.66 (1H, d, $J=8.9$ Hz), 7.36 (1H, dd, $J=8.9$, 2.1 Hz), 7.25 (1H, dd, $J=8.6$, 2.4 Hz), 7.10 (1H, d, $J=2.4$ Hz), 6.71 (1H, d, $J=8.6$ Hz), 6.39 (1H, d, $J=5.3$ Hz), 3.98 (2H, s), 3.33 (2H, m), 2.75 (2H, t, $J=6.9$ Hz), 1.79–1.85 (2H, m), 1.74–1.68 (2H, m). ^{13}C NMR (125 MHz, $\text{DMSO}-d_6$): δ 157.2, 152.3, 150.6, 149.7, 133.8, 131.2, 130.6, 128.0, 127.7, 124.5, 124.3, 118.0, 117.9, 109.9, 99.1, 50.2, 48.5, 42.8, 27.2, 26.2. IR (ATR, $\nu_{\text{max}}/\text{cm}^{-1}$): 3292, 3223, 3073, 2933, 2860, 1612 (7-chloroquinoline), 1578 (7-chloroquinoline), 1557 (7-chloroquinoline), 1470, 1451, 1432, 1396, 1383, 1368, 1358, 1337, 1319, 1257, 1207, 1178, 1165, 1142, 1121, 1111, 1080, 1039, 1014, 933, 981, 952, 898, 871, 846, 812, 800, 766, 740, 641, 622, 564.

2-(((4-((7-Chloroquinolin-4-yl)amino)butyl)amino)methyl)-4-methylphenol, 8b

8b was obtained from **8a** (92.0 mg, 0.25 mmol) and NaBH_4 (17.0 mg, 0.45 mmol). Yield: 96% (88 mg). mp: 163 °C. Elemental analysis (%) calcd. for $\text{C}_{21}\text{H}_{24}\text{ClN}_3\text{O}_1/6\text{CH}_2\text{Cl}_2$: C 66.20, H 6.39; N 10.94; found: C 66.40, H 6.15, N 10.61. ^1H NMR (500 MHz, CDCl_3): δ 8.46 (1H, d, $J=5.4$ Hz), 7.89 (1H, d, $J=2.1$ Hz), 7.60 (1H, d, $J=8.9$ Hz), 7.29 (1H, dd, $J=8.9$, 2.1 Hz), 6.91 (1H, dd, $J=8.2$, 2.4 Hz), 6.73 (1H, d, $J=2.4$ Hz), 6.67 (1H, d, $J=8.2$ Hz), 6.32 (1H, d, $J=5.4$ Hz), 3.91 (2H, s), 3.26 (2H, t, $J=7.0$ Hz), 2.70 (2H, t, $J=7.0$ Hz), 2.17 (3H, s), 1.80–1.74 (2H, m), 1.60–1.68 (2H, m). ^{13}C NMR (75 MHz, $\text{DMSO}-d_6$): δ 155.5, 152.3, 150.6, 149.7, 133.8, 129.5, 128.6, 128.0, 127.2, 124.5, 124.3, 124.3, 118.0, 115.7, 99.2, 51.1, 48.5, 42.9, 27.1, 26.2, 20.5. IR (ATR, $\nu_{\text{max}}/\text{cm}^{-1}$): 3271, 3216, 3020, 2949, 2922, 2877, 2837, 1611 (7-chloroquinoline), 1579 (7-chloroquinoline), 1546 (7-chloroquinoline), 1508, 1488, 1469, 1448, 1426, 1381, 1368, 1329, 1275, 1242, 1209, 1166, 1147, 1134, 1108, 1071, 1057, 1027, 1008, 983, 973, 957, 923, 897, 877, 854, 824, 812, 801, 778, 766, 747, 722, 655, 623, 604.

2-(((6-((7-Chloroquinolin-4-yl)amino)hexyl)amino)methyl)-phenol, 9b

9b was obtained from **9a** (191 mg, 0.50 mmol) and NaBH_4 (26.6 mg, 0.70 mmol). Yield: 69% (133 mg). mp: 76 °C. Elemental analysis (%) calcd. for $\text{C}_{22}\text{H}_{26}\text{ClN}_3\text{O}_1/4\text{CH}_2\text{Cl}_2$: C 65.96, H 6.59, N 10.37; found: C 66.40, H 6.56, N 10.16. ^1H NMR (500 MHz, CDCl_3): δ 8.45 (1H, d, $J=5.4$ Hz), 7.88 (1H, d, $J=2.1$ Hz), 7.61 (1H, d, $J=9.0$ Hz), 7.26 (1H, dd, $J=9.0$, 2.1 Hz), 7.12–7.08 (1H, td, $J=8.0$, 1.8 Hz), 6.92 (1H, dd, $J=7.6$, 1.8 Hz), 6.76 (1H, dd, $J=8.0$, 1.3 Hz), 6.71 (1H, td, $J=7.6$, 1.3 Hz), 6.33 (1H, d, $J=5.4$ Hz), 3.93 (2H, s), 3.22–3.26 (2H, m), 2.63 (2H, t, $J=6.9$ Hz), 1.73–1.66 (2H, m), 1.55–1.48 (2H, m), 1.39 (4H, m). ^{13}C NMR (75 MHz, $\text{DMSO}-d_6$): δ 158.2, 152.3, 150.7, 149.7, 133.8, 128.8, 128.2, 128.0, 124.6, 124.5, 124.3, 118.8, 118.1, 115.9, 99.1, 51.4, 48.6, 42.9, 29.4, 28.3, 27.0, 26.9. IR (ATR, $\nu_{\text{max}}/\text{cm}^{-1}$): 3264, 3061, 2938, 2859, 1613 (7-chloroquinoline), 1576 (7-chloroquinoline), 1542 (7-chloroquinoline), 1478, 1470, 1451, 1424, 1364, 1332, 1320, 1279, 1247, 1201, 1184, 1164, 1139, 1101, 1079, 1035, 997, 966, 927, 901, 885, 866, 846, 807, 760, 748, 718, 641, 621.

4-Bromo-2-(((6-((7-chloroquinolin-4-yl)amino)hexyl)amino)methyl)phenol, 10b

10b was obtained from **10a** (230 mg, 0.50 mmol) and NaBH_4 (26.6 mg, 0.70 mmol). Yield: 54% (126 mg). mp: 131 °C. Elemental analysis (%) calcd. for $\text{C}_{22}\text{H}_{25}\text{BrClN}_3\text{O}_1/4\text{CH}_2\text{Cl}_2$: C 55.21, H 5.31, N 8.68; found: C 55.51, H 5.23, N 8.80. ^1H NMR (500 MHz, CDCl_3): δ 8.44 (1H, d, $J=5.4$ Hz), 7.88 (1H, d, $J=2.1$ Hz), 7.60 (1H, d, $J=8.9$ Hz), 7.27 (1H, dd, $J=8.9$, 2.1 Hz), 7.18 (1H, dd, $J=8.6$, 2.4 Hz), 7.03 (1H, d, $J=2.4$ Hz), 6.63 (1H, d, $J=8.6$ Hz), 6.33 (1H, d, $J=5.4$ Hz), 3.89 (2H, s), 3.22–3.26 (2H, m), 2.61 (2H, t, $J=7.0$ Hz), 1.73–1.66 (2H, m), 1.54–1.47 (2H, m), 1.44–1.34 (4H, m). ^{13}C NMR (75 MHz, $\text{DMSO}-d_6$): δ 157.4, 152.3, 150.7, 149.7, 133.8, 131.2, 130.6, 128.0, 127.7, 124.5, 124.3, 118.0, 118.0, 109.8, 99.1, 50.4, 48.6, 42.9, 29.4, 28.3, 26.9. IR (ATR, $\nu_{\text{max}}/\text{cm}^{-1}$): 3265, 3200, 3058, 2929, 2879, 2851, 2813, 1611 (7-chloroquinoline), 1578 (7-chloroquinoline), 1543 (7-chloroquinoline), 1479, 1448, 1427, 1390, 1366, 1332, 1299, 1278, 1252, 1227, 1200, 1175, 1161, 1143, 1134, 1111, 1097, 1075, 1031, 1019, 980, 959, 936, 917, 895, 869, 818, 808, 763, 720, 637, 623, 602, 569, 548.

2-(((6-((7-Chloroquinolin-4-yl)amino)hexyl)amino)methyl)-4-methylphenol, 11b

11b was obtained from **11a** (119 mg, 0.30 mmol) and NaBH_4 (19.0 mg, 0.50 mmol). Yield: 95% (121 mg). mp: 131 °C. Elemental analysis (%) calcd. for $\text{C}_{23}\text{H}_{28}\text{ClN}_3\text{O}_1/2\text{H}_2\text{O}$: C 67.88, H 7.18, N 10.33; found: C 67.75, H 6.85, N 10.17. ^1H NMR (500 MHz, CDCl_3): δ 8.45 (1H, d, $J=5.4$ Hz), 7.88 (1H, d, $J=2.1$ Hz), 7.62 (1H, d, $J=9.0$ Hz), 7.26 (1H, dd, $J=9.0$, 2.1 Hz), 6.90 (1H, dd, $J=8.1$, 1.8 Hz), 6.73 (1H, d, $J=1.8$ Hz), 6.66 (1H, d, $J=8.1$ Hz), 6.34 (1H, d, $J=5.4$ Hz), 5.04 (1H, s), 3.88 (2H, s), 3.25 (2H, m), 2.62 (2H, t, $J=6.9$ Hz), 2.17 (3H, s), 1.73–1.66 (2H, m), 1.54–1.48 (2H, m), 1.45–1.34 (4H, m). ^{13}C NMR (75 MHz, $\text{DMSO}-d_6$): δ 155.0, 151.6, 149.9, 148.9, 133.1, 128.7, 127.8, 127.2, 126.4, 123.7, 123.6, 123.3, 117.3, 114.9, 98.3, 50.5, 47.8, 42.2, 28.6, 27.6, 26.2, 26.1, 19.8. IR (ATR, $\nu_{\text{max}}/\text{cm}^{-1}$): 3230, 3289,

3233, 3061, 2927, 2854, 1610 (7-chloroquinoline), 1577 (7-chloroquinoline), 1537 (7-chloroquinoline), 1497, 1449, 1427, 1366, 1331, 1279, 1250, 1214, 1203, 1170, 1136, 1079, 1005, 964, 937, 899, 876, 850, 807, 727, 643, 623, 599, 555.

Biological assays

Cholinesterase inhibitory activity

In order to determine the anticholinesterase activity, the modified Ellman's test (Lima et al., 2009) for a 96-well plate was used (Ellman et al., 1961). The velocities of substrate hydrolysis by AChE and BChE as function of sample concentration were evaluated for *EeAChE* and *EqBChE*. *EeAChE*, *EqBChE* and Ellman's reagent (5,5'-dithiobis-2-nitrobenzoic acid—DTNB) were prepared in phosphate buffer (100 mM, pH 7.4). Acetylthiocholine iodide (ATCI), and BTCl were prepared in distilled water. Stock samples (500 mM) were prepared in dimethyl sulfoxide (DMSO) or ethanol (only compound **9b**) and appropriately diluted in phosphate buffer to the desired concentrations immediately before use. All solutions were kept on ice during the experiments. All experiments were performed at $25^{\circ}\text{C} \pm 1^{\circ}\text{C}$. All experimental wells received *EeAChE* (0.01 U/mL) or *EqBChE* (0.05 U/mL), DTNB (0.25 mM), and phosphate buffer (control—activity) or sample solutions (0.01–100 μM). The mixture was incubated for 10 min. Then, ATCI (0.5 mM) or BTCl (1.0 mM) was added to all wells and the plate was read immediately during 5 min in a spectrophotometer (Spectramax 340PC, Molecular Device®). The spontaneous hydrolysis of the substrate was evaluated by replacing enzyme for buffer. The solvents (DMSO or ethanol) were evaluated at the highest concentration (0.2%) used in the experiment. All concentrations refer to the final values. The samples were tested in at least five different concentrations. The enzyme activity ($\text{absorbance} \cdot \text{min}^{-1}$) in a sample solution was determined by comparison with the control (mixture without sample) and expressed as the change in the optic deviation at 405 nm. *EeAChE*, *EqBChE*, ATCI, BTCl and DTNB were purchased from Sigma-Aldrich (Brazil).

Kinetics of enzyme inhibition

The same modified Ellman's test of spectrophotometric analysis was used to determine the type of inhibition. Kinetic parameters were determined using the Lineweaver–Burk double reciprocal method (Lineweaver & Burk, 1934) at increasing concentrations of substrate (0.1; 0.3; 0.5; 1.0; 1.5; 2.0 mM) below and above K_m , keeping a fixed amount of enzyme in the absence or in the presence of inhibitor. The inhibitors concentrations were kept close to one which corresponds to the IC_{50} and their inhibitory kinetics were evaluated by the Lineweaver and Burk method (Lineweaver & Burk, 1934).

Animals

This study was approved by the Ethics Committee of the Health Sciences Center at the Federal University of Rio de Janeiro (Universidade Federal do Rio de Janeiro, UFRJ;

protocol n.: A6/19-001-16). The 'Principles of laboratory animal care' (NIH publication No. 85–23, revised 1996; NIH, 2011) guidelines were strictly followed for all experiments. Swiss mice were obtained from the Biomedical Sciences Institute, UFRJ, Brazil).

Astrocyte cultures

Astrocyte cultures were prepared from mixed primary brain cultures obtained from the cerebral cortices of newborn mice (Lima et al., 2007). The primary brain cells were obtained by dissociating the cerebral cortices until they turned into a suspension of cells, which were cultivated in Dulbecco's modified Eagle medium/F12 (DMEM-F12) and supplemented with glucose (33 mM), glutamine (2 mM), sodium bicarbonate (3 mM), penicillin and streptomycin (0.5 $\text{mg} \cdot \text{mL}^{-1}$), Fungizone (2.5 $\text{g} \cdot \text{mL}^{-1}$) and 10% of fetal bovine serum (FBS, v/v) for 12 days (Lima et al., 2007). After this period, the cells were detached from the culture flasks by exposure to 0.25% Trypsin to obtain mostly astrocyte cells and they were seeded at the density required for the experiment. The cells were maintained at 37°C in 5% CO_2 and 95% air atmosphere. Astrocytes were identified by immunostaining using glial fibrillary acidic protein antibody (DAKO), attesting the efficiency of the culture method (not shown).

Maintenance of the N9 microglial lineage cells

The mice N9 microglial lineage cells were cultivated in DMEM-F12 with 10% FBS (v/v). The culture flasks were maintained at 37°C in 5% CO_2 and 95% air mixture. Cells displaying exponential growth were detached from the culture flasks with ethylene-diamine tetraacetic acid (EDTA) and seeded at the density required for the experiment.

MTT cytotoxicity assay

Cytotoxicity was assessed by the MTT (3-[4,5-dimethylthiazol-2-yl]-2,5-diphenyltetrazolium bromide) assay. Astrocytes were plated on a 96-well plate in a density of $1 \cdot 10^4$ cells per well with DMEM-F12 with 10% FBS. The next day the cells were washed three times with DMEM-F12 without serum and treated with different concentrations of the compounds based on the IC_{50} values of each compound for AChE and BChE as follows: **3b** (0.5, 2, 20, 30 and 60 μM), **5b** (0.5, 2 and 20 μM), **6b** (0.2, 0.6, 6, 8 and 16 μM), **8b** (0.2, 1, 8, 10 and 16 μM), **7b** (0.2, 1, 5 and 10 μM), **9b** (0.06, 0.3, 3, 10 and 30 μM), **11b** (0.06, 0.3, 3, 10 and 30 μM), **10b** (0.06, 0.3, 3, 10 and 30 μM), **9a** (0.2, 0.7, 7, 60 and 100 μM).

All compounds were dissolved in DMSO and then dissolved in serum-free DMEM-F12 to be incubated with the cells for 24 and 48 h. The viable cells were detected by the ability to convert MTT into insoluble formazan as previously described (Gardner, 1974). The absorption was measured at 595 nm relative to the control (serum-free DMEM-F12) using a Wallac Victor3 1420 Multilabel Counter of Perkin Elmer. Absorption at the reference wavelength was subtracted from the absorption at the test wavelength.

N9 microglial lineage production of NO

N9 cells were cultured in 96-well plate at the density of 5.10^4 cells per well and treated for 48 h with **9a** (7 μ M; 60 μ M), **5b** (10 μ M), **3b** (20 μ M; 30 μ M), **10b** (3 μ M; 10 μ M). The concentrations were based on the IC_{50} values for AChE and BChE, respectively, that did not present toxic effect on the astrocyte culture. LPS from *Escherichia coli* (Sigma; $1 \mu\text{g}\cdot\text{mL}^{-1}$) was used as positive control. Nitric Oxide (NO•) production was evaluated by determining the nitrite levels using the colorimetric Griess method (Sun et al., 2003).

Statistical analysis. The data were analyzed by one-way ANOVA, followed by Dunnett's multiple comparison test, using the software GraphPad Prism®. The results correspond to average with standard deviation of three experiments, each one made in triplicate.

Docking energy calculations

Aqueous equilibrium studies at pH 7.4 were performed on all ligands using the Chemicalize server (<https://chemicalize.com/>) in order to determine their protonation states under physiologic pH. The most abundant chemical species of each compound was, then, selected for the docking studies. Their tridimensional structures were constructed using the software PC Spartan Pro® (Hehre & Deppmeier, 1999) and their partial atomic charges were calculated through the RM1 (Recife Model 1) semi-empirical method (Rocha et al., 2006).

The structure EeAChE complexed with donepezil was constructed through homology modeling from the crystallographic structure of human AChE (HssAChE) complexed with donepezil, available in the RCSB PDB Protein Data Bank (<http://www.rcsb.org/pdb/home/home.do>), under the code 4EY7 (Cheung et al., 2012), while the structure of EqBChE, complexed with tacrine was built through homology modeling from the crystallographic structure of human BChE (HssBChE) complexed with tacrine, available in the RCSB PDB Protein Data Bank (<http://www.rcsb.org/pdb/home/home.do>), under the code 4BDS (Nachon et al., 2013).

The docking energies of the ligands inside the active sites of EeAChE and EqBChE, were obtained using the software Molegro Virtual Docker (MVD)® (Thomsen & Christensen, 2006). The docking grids for both enzymes were restricted into spheres with a radius of 12 Å centered on donepezil (for EeAChE) and tacrine (for EqBChE). Residues inside these spheres were considered flexible. Due to the stochastic nature of the docking algorithm, about 10 runs were performed for each compound with 30 poses (conformation and orientation of the ligand) returned to the analysis. This protocol was validated through re-docking of donepezil and tacrine over its experimental structures from HssAChE and HssBChE, respectively. The best pose of each compound inside EeAChE and EqBChE, was selected according to the lowest binding energies, the hydrogen bonds (H-bond) interactions observed and the superposition to donepezil (for EeAChE) or tacrine (for EqBChE).

Acknowledgments

We are grateful to the Molecular Spectroscopy (<http://www.uff.br/lame/>) and NMR (<http://www.laremn.uff.br>) Multiuser Laboratories at Universidade Federal Fluminense. We also thank the free software developers (Linux, Gromacs, VMD, Qtiplot, Xmgrace, etc.) who made our molecular modeling possible. T.C.C.F wish to thank the Military Institute of Engineering and the Federal University of Lavras for the software infrastructure. This work was also supported by the excellence project UHK.

Disclosure statement

No potential conflict of interest was reported by the authors.

Funding

The authors gratefully acknowledge the Brazilian Federal agencies Conselho Nacional de Desenvolvimento Científico e Tecnológico—CNPq (grant numbers 306136/2011-2—M.D.V. and 308225/2018-0—T.C.C.F.; fellowship—R.F.A), Coordenação de Aperfeiçoamento de Pessoal de Nível Superior—CAPES (fellowship—V.S.Z. and visiting professor fellowship—J.A.L.), National Institutes for Science and Technology (INCT-NT grant number 465346/2014-6—F.R.S.L.) and the Rio de Janeiro Research Foundation (FAPERJ, grant numbers 26/201.352/2014—M.D.V., 02/202.961/2017—T.C.C.F.).

ORCID

Vanessa S. Zanon  <http://orcid.org/0000-0002-3554-9496>
 Josélia A. Lima  <http://orcid.org/0000-0002-2076-1144>
 Rackele F. Amaral  <http://orcid.org/0000-0001-7645-9086>
 Flavia R. S. Lima  <http://orcid.org/0000-0003-0799-9235>
 Daniel A. S. Kitagawa  <http://orcid.org/0000-0002-6298-0492>
 Tanos C. C. França  <http://orcid.org/0000-0002-6048-8103>
 Maria D. Vargas  <http://orcid.org/0000-0002-8881-824X>

References

- Caldwell, C. C., Yao, J., & Brinton, R. D. (2015). Targeting the prodromal stage of Alzheimer's Disease: Bioenergetic and mitochondrial opportunities. *Neurotherapeutics*, 12(1), 66–80. <https://doi.org/10.1007/s13311-014-0324-8>
- Chen, Y., Bian, Y., Sun, Y., Kang, C., Yu, S., Fu, T., Li, W., Pei, Y., & Sun, H. (2016). Identification of 4-aminoquinoline core for the design of new cholinesterase inhibitors. *PeerJ*, 4, e2140. <https://doi.org/10.7717/peerj.2140>
- Cheung, J., Rudolph, M. J., Burshteyn, F., Cassidy, M. S., Gary, E. N., Love, J., Franklin, M. C., & Height, J. J. (2012). Structures of human acetylcholinesterase in complex with pharmacologically important ligands. *Journal of Medicinal Chemistry*, 55(22), 10282–10286. <http://www.ncbi.nlm.nih.gov/pubmed/23035744>.
- Daina, A., Michielin, O., & Zoete, V. (2017). SwissADME: A free web tool to evaluate pharmacokinetics, drug-likeness and medicinal chemistry friendliness of small molecules. *Scientific Reports*, 7(1), 42717–42713. <https://doi.org/10.1038/srep42717>
- Ekengard, E., Glans, L., Cassells, I., Fogeron, T., Govender, P., Stringer, T., Chellan, P., Lisensky, G. C., Hersh, W. H., Doverbratt, I., Lidin, S., de Kock, C., Smith, P. J., Smith, G. S., & Nordlander, E. (2015). Antimalarial activity of ruthenium(II) and osmium(II) arene complexes with mono- and bidentate chloroquine analogue ligands. *Dalton Transactions (Cambridge, England: 2003)*, 44(44), 19314–19329. <https://doi.org/10.1039/C5DT02410B>
- Ellman, G. L., Courtney, K. D., Andres, V., & Feather-Stone, R. M. (1961). A new and rapid colorimetric determination of acetylcholinesterase

- activity. *Biochemical Pharmacology*, 7(2), 88–95. [https://doi.org/10.1016/0006-2952\(61\)90145-9](https://doi.org/10.1016/0006-2952(61)90145-9)
- Fernández-Bachiller, M. I., Pérez, C., Monjas, L., Rademann, J., & Rodríguez-Franco, M. I. (2012). New Tacrine-4-Oxo-4H-Chromene hybrids as multifunctional agents for the treatment of Alzheimer's disease, with cholinergic, antioxidant, and β -amyloid-reducing properties. *Journal of Medicinal Chemistry*, 55(3), 1303–1317. <https://doi.org/10.1021/jm201460y>
- Gardner, R. S. (1974). A sensitive colorimetric assay for mitochondrial α -glycerophosphate dehydrogenase. *Analytical Biochemistry*, 59(1), 272–276. [https://doi.org/10.1016/0003-2697\(74\)90033-5](https://doi.org/10.1016/0003-2697(74)90033-5)
- Greig, N. H., Utsuki, T., Yu, Q., Zhu, X., Holloway, H. W., Perry, T., Lee, B., Ingram, D. K., & Lahiri, D. K. (2001). A new therapeutic target in Alzheimer's disease treatment: Attention to butyrylcholinesterase. *Current Medical Research and Opinion*, 17(3), 159–165. <https://doi.org/10.1185/03007990152673800>
- Guillozet, A. L., Mesulam, M.-M., Smiley, J. F., & Mash, D. C. (1997). Butyrylcholinesterase in the life cycle of amyloid plaques. *Annals of Neurology*, 42(6), 909–918. <https://doi.org/10.1002/ana.410420613>
- Guzmán-Martínez, L., Farías, G. A., & Maccioni, R. B. (2013). Tau oligomers as potential targets for Alzheimer's diagnosis and novel drugs. *Frontiers in Neurology*, 4, 167. <http://journal.frontiersin.org/article/10.3389/fneur.2013.00167/abstract>
- Hastings, I. M., Bray, P. G., & Ward, S. A. (2002). Parasitology: A requiem for chloroquine. *Science (New York, N.Y.)*, 298(5591), 74–75. <https://doi.org/10.1126/science.1077573>
- Hehre, W. J., & Deppmeier, B. J. (1999). *PC SPARTAN Pro. Wavefunction, Inc., Irvine, 1999*. Wavefunction.
- Ikram, M., Saeed-Ur-Rehman, S., Rehman, R. J., Baker, C., & Schulzke, (2012). Synthesis, characterization and distinct butyrylcholinesterase activities of transition metal complexes of 2-[(E)-(Quinolin-3-Ylimino)Methyl]Phenol. *Inorganica Chimica Acta*, 390, 210–216. <https://doi.org/10.1016/j.ica.2012.04.036>
- Kontoyianni, M., McClellan, L. M., & Sokol, G. S. (2004). Evaluation of docking performance: Comparative data on docking algorithms. *Journal of Medicinal Chemistry*, 47(3), 558–565. <http://www.ncbi.nlm.nih.gov/pubmed/14736237>
- Kumar, S., Bawa, S., & Gupta, H. (2009). Biological activities of quinoline derivatives. *Mini Reviews in Medicinal Chemistry*, 9(14), 1648–1654. <http://www.eurekaselect.com/openurl/content.php?genre=article&issn=1389-5575&volume=9&issue=14&page=1648>
- Li, F., Wang, Z. M., Wu, J. J., Wang, J., Xie, S. S., Lan, J. S., Xu, W., Kong, L. Y., & Wang, X. B. (2016). Synthesis and pharmacological evaluation of donepezil-based agents as new cholinesterase/monoamine oxidase inhibitors for the potential application against Alzheimer's disease. *Journal of Enzyme Inhibition and Medicinal Chemistry*, 31(sup3), 41–53. <https://www.tandfonline.com/doi/full/10.1080/14756366.2016.1201814>
- Lima, F. R., Arantes, C., Muras, A. G., Nomizo, R., Brentani, R. R., & Martins, V. R. (2007). Cellular prion protein expression in astrocytes modulates neuronal survival and differentiation. *Journal of Neurochemistry*, 103(6), 2164–2176. <http://doi.wiley.com/10.1111/j.1471-4159.2007.04904.x>
- Lima, J. A., Costa, R. S., Epifânio, R. A., Castro, N. G., Rocha, M. S., & Pinto, A. C. (2009). Geissospermum Vellozii Stembark. *Pharmacology Biochemistry and Behavior*, 92(3), 508–513. <https://doi.org/10.1016/j.pbb.2009.01.024>
- Lineweaver, H., & Burk, D. (1934). The determination of enzyme dissociation constants. *Journal of the American Chemical Society*, 56(3), 658–666. <https://doi.org/10.1021/ja01318a036>
- Mantoani, S., Chierrito, T., Vilela, A., Cardoso, C., Martínez, A., & Carvalho, I. (2016). Novel triazole-quinoline derivatives as selective dual binding site acetylcholinesterase inhibitors. *Molecules*, 21(2), 193. <https://www.mdpi.com/1420-3049/21/2/193>
- Mao, F., Huang, L., Luo, Z., Liu, A., Lu, C., Xie, Z., & Li, X. (2012). O-hydroxyl- or o-amino benzylamine-tacrine hybrids: Multifunctional biomaterials chelators, antioxidants, and inhibitors of cholinesterase activity and amyloid- β aggregation. *Bioorganic & Medicinal Chemistry*, 20(19), 5884–5892. <https://doi.org/10.1016/j.bmc.2012.07.045>
- Marella, A., Tanwar, O. P., Saha, R., Ali, M. R., Srivastava, S., Akhter, M., Shaquiquzzaman, M., & Alam, M. M. (2013). Quinoline: A versatile heterocyclic. *Saudi Pharmaceutical Journal*, 21(1), 1–12. <https://doi.org/10.1016/j.jsps.2012.03.002>
- Mesulam, M. M. (2009). Acetylcholine neurotransmission in CNS. In *Encyclopedia of Neuroscience*, 1–4. Elsevier Ltd.
- Millington, C., Sonogo, S., Karunaweera, N., Rangel, A., Aldrich-Wright, J. R., Campbell, I. L., Gyengesi, E., & Münch, G. (2014). Chronic neuroinflammation in Alzheimer's disease: New perspectives on animal models and promising candidate drugs. *BioMed Research International*, 2014, 309129–309110. <https://doi.org/10.1155/2014/309129>
- Nachon, F., Carletti, E., Ronco, C., Trovaslet, M., Nicolet, Y., Jean, L., & Renard, P. Y. (2013). Crystal structures of human cholinesterases in complex with huprine W and tacrine: Elements of specificity for anti-Alzheimer's drugs targeting acetyl- and butyryl-cholinesterase. *The Biochemical Journal*, 453(3), 393–399. <https://doi.org/10.1042/BJ20130013>
- Natarajan, J. K., Alumasa, J. N., Yearick, K., Ekoue-Kovi, K. A., Casabianca, L. B., de Dios, A. C., Wolf, C., & Roepe, P. D. (2008). 4-N-, 4-S-, and 4-O-chloroquine analogues: Influence of side chain length and quinolyl nitrogen pKa on activity vs chloroquine resistant malaria. *Journal of Medicinal Chemistry*, 51(12), 3466–3479. <https://doi.org/10.1021/jm701478a>
- Nuthakki, V. K., Mudududda, R., Sharma, A., Kumar, A., & Bharate, S. B. (2019). Synthesis and biological evaluation of indoloquinoline alkaloid cryptolepine and its bromo-derivative as dual cholinesterase inhibitors. *Bioorganic Chemistry*, 90, 103062. <https://doi.org/10.1016/j.bioorg.2019.103062>
- NIH (2011). *Guide for the care and use of Laboratory animals*. 8th ed. National Academy of Sciences. <https://grants.nih.gov/grants/olaw/guide-for-the-care-and-use-of-laboratory-animals.pdf>
- Özturan Özer, E., Unsal Tan, O., Ozadali, K., Küçükilinc, T., Balkan, A., & Uçar, G. (2013). Synthesis, molecular modeling and evaluation of novel N'-2-(4-benzylpiperidin-piperazin-1-yl)acylhydrazones as dual inhibitors for cholinesterases and A β aggregation. *Bioorganic & Medical Chemistry Letters*, 23(2), 440–443. <https://doi.org/10.1016/j.bmcl.2012.11.064>
- Pajouhesh, H., & Lenz, G. R. (2005). Medicinal chemical properties of successful central nervous system drugs. *NeuroRx: The Journal of the American Society for Experimental Neurotherapeutics*, 2(4), 541–553. <http://www.ncbi.nlm.nih.gov/pubmed/16489364>
- Reyes, A. E., Chacón, M. A., Dinamarca, M. C., Cerpa, W., Morgan, C., & Inestrosa, N. C. (2004). Acetylcholinesterase-A beta complexes are more toxic than A beta fibrils in rat hippocampus: Effect on rat beta-amyloid aggregation, laminin expression, reactive astrocytosis, and neuronal cell loss. *The American Journal of Pathology*, 164(6), 2163–2174. [https://doi.org/10.1016/s0002-9440\(10\)63774-1](https://doi.org/10.1016/s0002-9440(10)63774-1)
- Rocha, G. B., Freire, R. O., Simas, A. M., & Stewart, J. J. P. (2006). RM1: A Reparameterization of AM1 for H, C, N, O, P, S, F, Cl, Br, and I. *Journal of Computational Chemistry*, 27(10), 1101–1111. <http://www.ncbi.nlm.nih.gov/pubmed/16691568>
- Stellwagen, D., Kemp, G. M., Valade, S., & Chambon, J. (2019). Glial regulation of synaptic function in models of addiction. *Current Opinion in Neurobiology*, 57, 179–185. <https://doi.org/10.1016/j.conb.2019.02.010>
- Sun, J., Zhang, X., Broderick, M., & Fein, H. (2003). Measurement of nitric oxide production in biological systems by using griess reaction assay. *Sensors*, 3(8), 276–284. <http://www.mdpi.com/1424-8220/3/8/276>
- Thomsen, R., & Christensen, M. H. M. H. (2006). MolDock: A new technique for high-accuracy molecular docking. *Journal of Medicinal Chemistry*, 49(11), 3315–3321. <http://www.ncbi.nlm.nih.gov/pubmed/16722650>
- Valori, C. F., Guidotti, G., Brambilla, L., & Rossi, D. (2019). Astrocytes: Emerging therapeutic targets in neurological disorders. *Trends in Molecular Medicine*, 25(9), 750–759. <https://doi.org/10.1016/j.molmed.2019.04.010>
- Wyss-Coray, T., & Mucke, L. (2002). Inflammation in neurodegenerative disease—A double-edged sword. *Neuron*, 35(3), 419–432. [https://doi.org/10.1016/S0896-6273\(02\)00794-8](https://doi.org/10.1016/S0896-6273(02)00794-8)
- Zanon, V. S., Lima, J. A., Cuya, T., Lima, F. R. S., da Fonseca, A. C. C., Gomez, J. G., Ribeiro, R. R., França, T. C. C., & Vargas, M. D. (2019). In-vitro evaluation studies of 7-chloro-4-aminoquinoline Schiff bases and their copper complexes as cholinesterase inhibitors. *Journal of Inorganic Biochemistry*, 191, 183–193. <https://doi.org/10.1016/j.jinorgbio.2018.11.019>